Korean J. of Chem. Eng., **14**(2), 129-135 (1997)

EVALUATION OF NUCLEATION ACTIVATION ENERGY IN METAL CVD PROCESSES

Jaesung Han† **and Klavs F. Jensen***

Taedok Institute of Technology, Yukong Limited, Yusung-Gu, Taejon 305-370, Korea
*Department of Chemical Engineering, Massachusetts Institute of Technology, Cambridge, MA 02139, U.S.A.
(Received 3 December 1996 • accepted 20 March 1997)

Abstract – A new approach to evaluate activation energy for nucleation in metal chemical vapor deposition (CVD) is presented. Deposition is performed by laser induced chemical vapor deposition (LCVD) using a low laser power and a high scan speed, so that only discrete particles in the initial nucleation stage are formed. The nucleation activation energy is then obtained from a relationship between the laser-induced surface temperature distribution and the particle distribution. The activation energy is directly related to the nucleation barrier, and hence the difference in the nucleation activation energies on different substrates may be used to explain the chemical selectivity which is often observed during metal CVD processes. This approach is experimentally applied to aluminum CVD using dimethylethylamine alane (DMEAA) precursor, and its nucleation activation energy is found to be 25kcal/mol on silicon surface.

Key words : Laser, CVD, Nucleation, Selectivity, DMEAA

INTRODUCTION

Properties of a thin film material deposited on a heterogeneous substrate, either by physical condensation or chemical vapor deposition, are strongly influenced by the initial nucleation phase. Naturally, understanding the nucleation process has been one of the major issues in materials processing, and a significant number of experimental or theoretical studies have been conducted to delineate the underlying mechanisms governing the nucleation process. Unfortunately, most of nucleation studies have been conducted on physical vapor deposition by condensation [Venebles et al., 1973] and very little is known about nucleation phenomena in chemical vapor deposition. This discrepancy is partly due to the traditional importance of the physical vapor deposition in thin film deposition, and partly because of the complexity of the analysis when the nucleation involves surface reactions.

In this study, nucleation phenomena in metal CVD were investigated by a simplified analysis introducing an overall activation energy for nucleation. The overall activation energy accounts for various mechanisms leading to the formation of stable nuclei: *i.e.*, surface reactions leading to unstable metal monomers, desorption and surface diffusion, and formation of critical nuclei by coalescence. By comparing the difference of the nucleation activation energies on different substrate surfaces, the chemical selectivity of deposition may be quantitatively rationalized. A similar approach has recently been reported for aluminum deposition for TIBA (triisobutylaluminum) using a conventional large area CVD [Lee et al., 1993]. They observed a significant difference between nucleation activation energy on silicon surface and that on SiO_2 surface, which they concluded leads to the selective deposition toward silicon surface. Although studying the nucleation process by the conventional CVD is simple and straightforward, it is not easy to accomplish an exact control of dwell time of the surface under an elevated temperatures, due to the time delays for heating and quenching of the substrate. Besides, it is very likely that a mass transfer film is formed above the surface rendering actual precursor concentration in the reaction zone different from the bulk concentration.

In LCVD, however, the surface temperature distribution is established in less than 1 msec [Rantala et al., 1989], and by using a constant scan speed, the dwell time at elevated surface temperature may be precisely controlled. Also, the mass transfer limitation is negligible since the reaction is confined in a micron-sized spot. Therefore LCVD is a useful tool to investigate the nucleation phenomena occurring in chemical vapor deposition.

THEORETICAL BACKGROUND

The initiation of thin film growth in a pyrolytic chemical vapor deposition is composed of four different kinetic behaviors:

(1) Creation of unstable monomers (chemical reaction)
(2) Formation of stable nuclei (nucleation)
(3) Growth on the existing nuclei (growth)
(4) Agglomeration between particles (coalescence)

Fig. 1 shows a schematic description of the process, leading to the early stage of film growth. Since growth and coalescence take place simultaneously, a micrograph would show the final stage of nucleation [Fig. 1(d)]. Therefore it is necessary to relate the nucleation rate to the properties of the deposit which can be actually measured, such as number of particles per unit area or surface coverage by the particles. The number of particles is dependent on (2) nucleation and (4) coalescence, whereas, assuming two-dimensional coalescence, the surface coverage is dependent on (2) nucleation and (3) growth. Therefore,

†To whom all correspondence should be addressed.

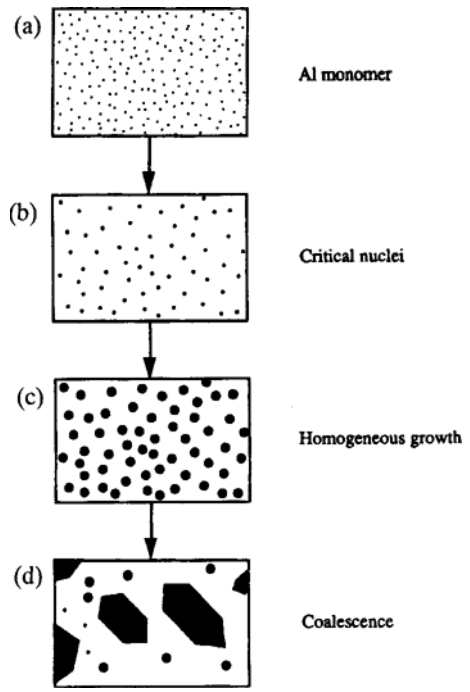

Fig. 1. Schematic description of initial nucleation process in chemical vapor deposition.

$$\frac{dN_P}{dt} = r_N - r_C \tag{1}$$

$$\frac{dF}{dt} = r_N \pi \phi_N^2 + r_G \sum_j^{N_r} (2\pi\phi_j) \tag{2}$$

The rate of formation of critical nuclei has been given for the case of film formation by physical condensation of the vapor phase [Venebles et al., 1984] as

$$r_N = r_m a_0 \varphi N_0 \left(\frac{r_m}{\nu_1 N_0}\right)^i \exp\left[\frac{(i+1)E_a + E_i - E_d}{RT}\right] \tag{3}$$

For chemical vapor deposition, the rate of monomer formation, r_m, is the surface reaction rate forming the monomer deposit, which can be assumed to be an Arrhenius type equation with activation energy (E_m) and pre-exponential factor (k_m).

$$r_m = k_m \exp(-E_m/RT) \tag{4}$$

Using Eq. (4) and rearranging Eq. (3), the nucleation rate (r_N) can be expressed in terms of overall activation energy (E_N) and overall pre-exponential factor (k_N) as follows.

$$r_N = k_N \exp(-E_N/RT) \tag{5}$$

with

$$k_N = k_m a_0 \varphi N_0 \left(\frac{k_m}{\nu_1 N_0}\right)^i \tag{6}$$

$$E_N = (i+1)(E_a + E_m) + E_i - E_d \tag{7}$$

Once a stable nucleus is formed, its size gets bigger either by coalescence with other particles or by the homogeneous growth on top of the nucleus. This section considers the homogeneous growth only. Assuming a hemispherical growth, the rate of increase in the radius of the particle is given as follows [Dubois et al., 1990]:

$$r_G[cm/s] = \frac{\gamma A n_s \exp(-E_a/RT)}{(An_s/\sigma S_r)\exp(-E_a/RT)+1} \tag{8}$$

Symbols used in this equation is defined in the reference, and $\gamma[=M_{Al}/N_{av}\rho_{Al}]$ is a constant converting the number of aluminum atoms deposited on a particle to the increase in the particle radius. However, since nucleation studies are typically conducted using moderate surface temperatures in order to avoid excessive growth, the growth is mostly governed by surface reaction rather than by adsorption of the precursor molecules. Therefore, for nucleation study, Eq. (8) can be simplified as

$$r_G \approx k_G \exp(-E_G/RT) \tag{9}$$

with $k_G=\gamma An_s$ and $E_G=E_a$.

1. Application to LCVD

The general knowledge about nucleation and growth kinetics is now extended to LCVD. The coordination system used in this section is same as in Fig. 1. The laser beam is scanning in the x-direction with a velocity, v_x. The y-coordinate designates the direction along the surface perpendicular to the laser travel. Total number of critical nuclei created per laser scan, N_∞, is given as the following integral equation:

$$N_\infty = \int_{scan} r_N dt_N = \int_{scan} k_N \exp(-E_N/RT_s) dt_N \tag{10}$$

Nucleation takes place only in the region where the surface temperature is higher than the nucleation threshold temperature. The nucleation threshold temperature for the aluminum precursor used in this study, DMEAA (dimethylethylamine alane), is not known, but assuming it is close to that of TMAA (trimethylamine alane), it may be approximately 100°C [Foulon and Stuke, 1993]. In the nucleation stage, the thermal effect of the aluminum deposit on determining the surface temperature is negligible, hence the analytical solution for the laser-induced temperature rise for a single homogeneous substrate [Lax, 1981] with a modified surface reflectivity is used to obtain the surface temperature distribution. Modification of the surface reflectivity is based on the average surface coverage by the aluminum particles in the laser spot. The incremental time, dt_N, can be converted to incremental displacement of the surface divided by the scan speed, dx/v_x, since the laser scans along x-direction with a constant speed, v_x. Also, the surface temperature distribution is symmetric with respect to x. Therefore, Eq. (10) can be rewritten as

$$N_\infty(y) = \frac{2k_N}{v_x}\int_0^{x(T_i)} \exp[-E_N/RT_s(x, y)]dx \tag{11}$$

where T_i is the threshold temperature for nucleation and $x(T_i)$ is the location of it. N_∞ has a distribution along y-direction.

However, since the actual particle distribution is determined also by coalescence and growth of the particles, the nucleation distribution given in Eq. (11) cannot be directly compared to those observed by SEM pictures. In order to simplify the analysis, two

different extremes are considered: (1) effect of the homogeneous growth is negligible and the particle size is predominantly determined by coalescence between particles; (2) effect of the coalescence is negligible and the particle size is predominantly determined by the homogeneous growth on top of the existing particle. Case (1) can be a reasonable assumption for nucleation on silicon or metal surfaces where the particles are small and densely distributed, and case (2) for nucleation on SiO_2 surfaces where the particles are very big and sparsely distributed.

2. Case (1): Growth is Negligible

If the homogeneous growth is suppressed by using a high scanning speed, the increase in the size of particles are purely from coalescence and that by growth is negligible. In this case, the number of particles will change, but, assuming the agglomeration of particles by the coalescence is two-dimensional, the total surface area covered by the deposit remains the same; *i.e.*,

$$F=\sum_{j}^{N_{obs}}\pi\phi_j^2=N_\infty\cdot(\pi\phi_N^2) \tag{12}$$

F is the fraction of substrate surface covered by the particles N_{obs} and ϕ_j's are the actual number and the two-dimensional radii of particles after coalescence, respectively. ϕ_N is the radius of the critical nucleus. From Eqs. (11) and (12), the surface coverage can be related to the surface temperature distribution as

$$F(y)=\frac{2\pi\phi_N^2 k_N}{v_x}\int_0^{x(T_i)}\exp[-E_N/RT_s(x,y)]dx \tag{13}$$

At a given laser power, the surface temperature is calculated by Lax's analytical solution, and by comparing the computed F (y) with the actual surface coverage distribution, the kinetic constants for the nucleation are obtained. The above analysis is valid only if the scan speed is high enough to suppress the additional growth on the existing particles.

3. Case (2): Coalescence is Negligible

When there is no coalescence between nuclei, the total number of nuclei is preserved. Therefore, the nucleation distribution given in Eq. (11) can be directly used for obtaining the nucleation kinetics. In addition, by analyzing the surface coverage by the particles, the kinetic information on nucleation may be correlated to that for growth. The surface coverage is the sum of the area occupied by each particle.

$$F=\sum_{j=1}^{N_\infty}\pi\phi_j^2=\pi\overline{\phi^2}N_\infty \tag{14}$$

ϕ_j is the radius of each particle and $\overline{\phi^2}$ is the geometric average of ϕ_j^2.

$$\overline{\phi^2}=\frac{\int_{T_s>T_i}\phi^2(t_N)k_N\exp(-E_N/RT_s)dt_N}{\int_{T_s>T_i}k_N\exp(-E_N/RT_s)dt_N} \tag{15}$$

where,

$$\phi(t_N)=\int_{t_N}^{\infty}r_G\,dt+\phi_N \tag{16}$$

where t_N is the time when each particle is born, r_G is the radial growth rate given in Eq. (8), and ϕ_N is the size of the critical nucleus which is negligible compared to the size of grown-up particles. Therefore, by combining Eqs (14)-(16), the surface coverage is related to the surface temperature as follows:

$$F(y)=\frac{\phi k_N k_G^2}{v_x^3}\int_{-x(T_i)}^{x(T_i)}\left[\int_{x_N}^{\infty}\exp(-E_G/RT_s)dx\right]^2\exp(-E_N/RT_s)dx_N \tag{17}$$

Again the relation $dt=dx/v_x$ is used to convert a time to a corresponding position along x-axis; accordingly x_N is the position where each particle is born. Assuming the kinetic constants for growth (k_G, E_G) and threshold temperature for nucleation (T_i) on the substrate are known, kinetic constants for nucleation (k_N, E_N) may be obtained by comparing the experimentally measured surface coverage distribution to that obtained by Eq. (17).

RESULTS AND DISCUSSION

1. Nucleation Induction Time

Eqs. (11), (13), (15), and (17) are valid only when the nucleation induction time (sometimes called incubation time) is much smaller than the surface residence time ($=2\omega/v_x$) at the laser heated region. Therefore, before using the concept to obtain the nucleation kinetics, it is necessary to check the nucleation induction time. LCVD was again used to estimate the induction time, and the main idea is to keep increasing the laser scan speed (v_x) until no deposition is observed. Fig. 2 shows the thickness of aluminum deposit on gold, platinum, (100)Si, and SiO_2 surfaces as a function of $2\omega/v_x$. Gold and platinum surfaces were prepared by coating 0.2 μm of the respective metal on (100)Si substrates by evaporation. A thermally grown 2 μm oxide layer on a (100)Si substrate was used as the SiO_2 surface. The thickness of the aluminum deposit was measured by Dektak. By extrapolating the thickness to zero, the minimum residence time for induc-

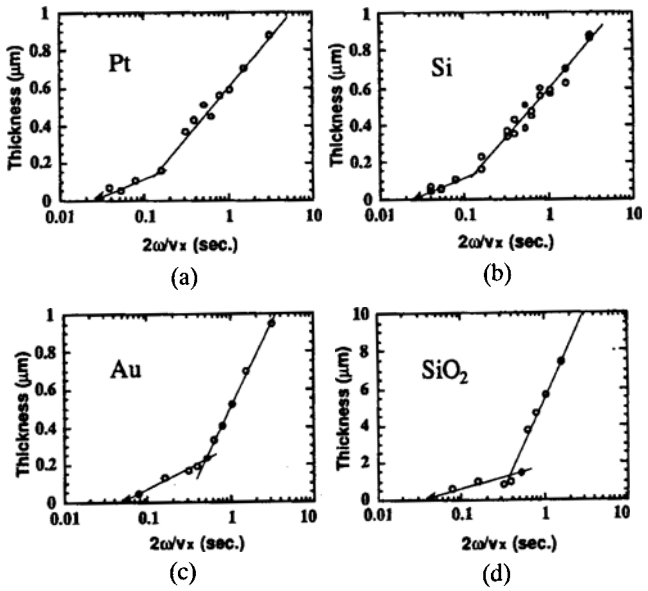

Fig. 2. Evaluation of nucleation induction time for aluminum LCVD from DMEAA on different surfaces: (a) Pt, (b) Au, (c) Si, and (d) SiO_2.

ing deposition was obtained, which was approximated to the nucleation induction time.

The nucleation induction time was about 2×10^{-2} second on silicon surfaces and was approximately the same order of magnitude on other surfaces, which are close to what has been reported for growth with TMAA (10^{-3} second) [Foulon and Stuke, 1993]. These value are sufficiently smaller than the laser residence time (~0.3 second) under normal operating conditions, and hence the approach developed in the previous section may be safely implemented. The thicknesses shown in Fig. 2 for different substrates cannot be directly compared with each other because the surface temperature rise is different on each substrate with the same laser power and scan speed. Growth rates on the SiO_2 surface appears to be much higher than those on other surfaces, but it is because of the insulating effect of the oxide layer increasing the temperature of the aluminum deposit.

2. Nucleation Activation Energies

First, nucleation on silicon surfaces was investigated. A high scan speed (100 μm/s) and low laser powers (1.2 to 1.5 kW/cm) were used to induce only nucleation while suppressing subsequent growth of bulk aluminum. Fig. 3 shows SEM pictures of the nucleated particles on a (100)Si substrate at different laser powers and Fig. 4 at different scan speeds. An environmental SEM which does not require coating of conductive material-gold, for example-was used to maintain the resolution. As the laser power was increased, the number of particles in unit area as well as the size of the each particle was increased. The total number and sizes of the particles are determined by three different mechanism occurring simultaneously-nucleation, growth, and coalescence. If the growth is negligible Eq. (13) can be used to get the nucleation kinetic constants, whereas if sintering is negligible, Eq. (17) is appropriate.

The relative importance of homogeneous growth and coalescence can be compared by estimating the net contribution of the homogeneous growth to the actual increase in particle size. According to Eq. (8), the linear growth rates of aluminum on aluminum surface is approximately 300 Å/s at this power level. With a scan speed of 100 μm/s and the beam diameter of 16 μm, the mean residence time under the laser is approximately 0.16 seconds, and hence the increase in particle radius by the homogeneous growth is only about 50 Å. This growth is negligible compared to the average radius of particles ranging from few hundreds to few thousand Å. It indicates that the increase in particle size has been predominantly by sintering rather than by growth. This is further illustrated by plotting a distribution of the particle number density across y-direction (Fig. 5). At higher laser power, a decrease in the number density is noticeable at the center of the laser beam as a result of the coalescence between particles.

Therefore, Eq. (13) is appropriate for analyzing the nucleation of aluminum on silicon substrates under the operating conditions used. The distribution of the surface coverage by the aluminum particles is calculated by the equation, and compared with that measured from Fig. 3 by an image analysis technique (Fig. 6). Kinetic parameters for nucleation (k_N, E_N) could be determined iteratively by a fit of the calculated distribution to the measured one. Resulting parameters are:

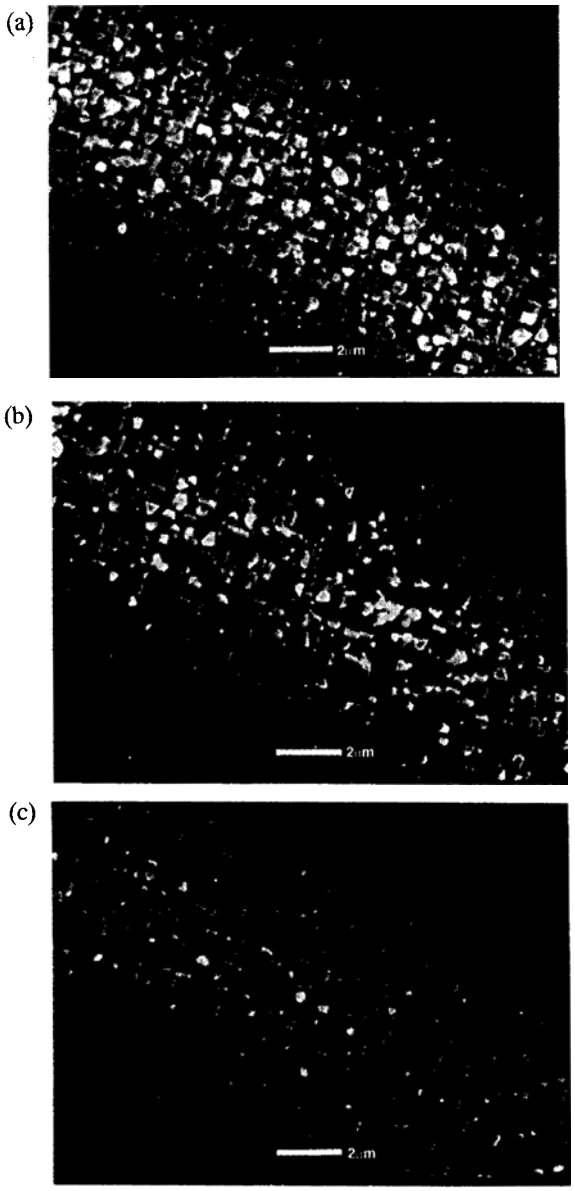

Fig. 3. SEM micrographs of aluminum grains formed on a silicon substrate at decreasing laser powers. Laser spot radius and scan speed were 8 μm and 100 μm/s, respectively; incident laser power was: (a) 1.17W, (b) 1.08W, and (c) 1.00W.

$$k_N(\#/cm^2s)=\frac{8\times10^{25}}{\phi_N^2},\qquad \phi_N \text{ is in Å} \tag{18}$$

$$E_N(kcal/mole)=25 \tag{19}$$

ϕ_N is the radius of the critical nucleus. The nucleation activation energy (25 kcal/mole) is higher than the homogeneous growth activation energy (~17.8 kcal/mole) [Dubois et al., 1990], which is believed to be the reason for the three-dimensional island growth. Also, assuming that the activation energy for homogeneous growth is approximately equal to the nucleation activation energy on metal surfaces, the difference may account for the selectivity of aluminum deposition toward metal in the pres-

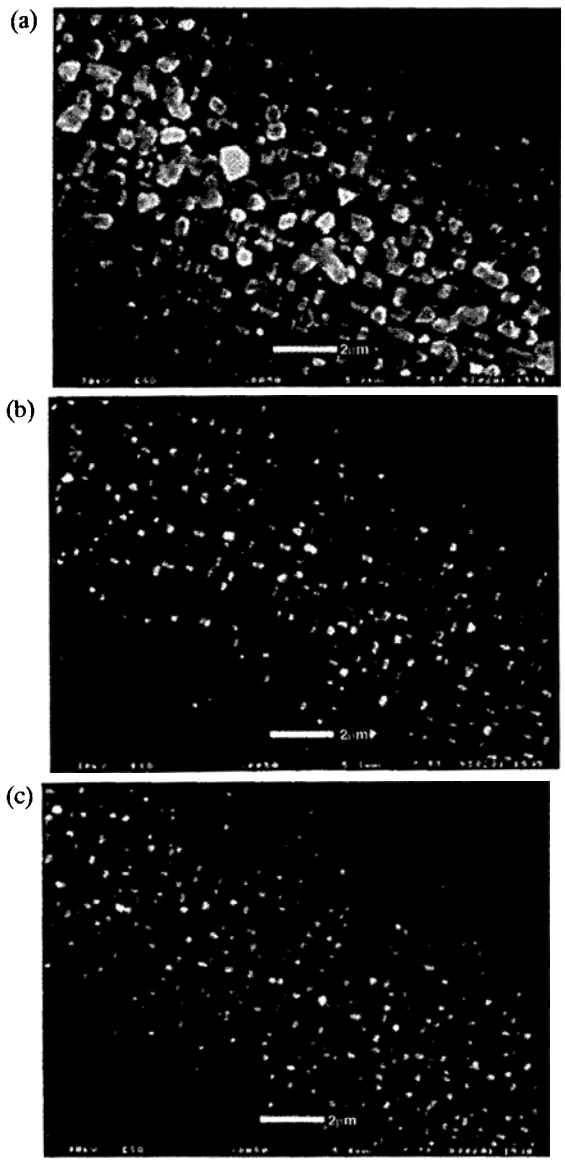

Fig. 4. SEM micrographs of aluminum grains formed on a silicon substrate at increasing laser scan speeds. Incident laser power and spot radius were 0.86W and 8 μm, respectively; scan speed was: (a) 10 μm/s, (b) 20 μm/s, and (c) 100 μm/s.

ence of silicon.

With the same operating conditions, the size of the deposited particles appeared to be smaller (~few hundred Å) on metal surfaces than those observed on silicon substrates. This indicates that the nucleation activation energy is lower on metal surfaces than on silicon surfaces. Unfortunately, SEM micrographs of the particles could not be obtained, because the strong secondary electron intensity of the background metal surface made it impossible to resolve the tiny aluminum particles. Possible alternative way to get the particle distribution would be analysis by TEM (transmission electron microscope), AFM (atomic force microscope), or EDX (emission diffraction X-ray).

Although quantitative analyses of nucleation kinetics on the metal surfaces could not be performed, it seems reasonable to assume that the nucleation activation energy is similar to the growth

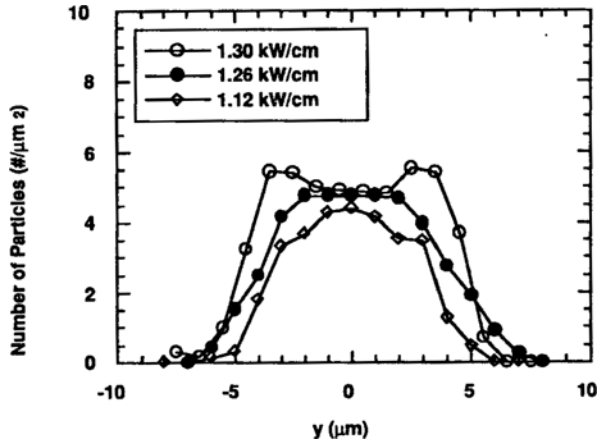

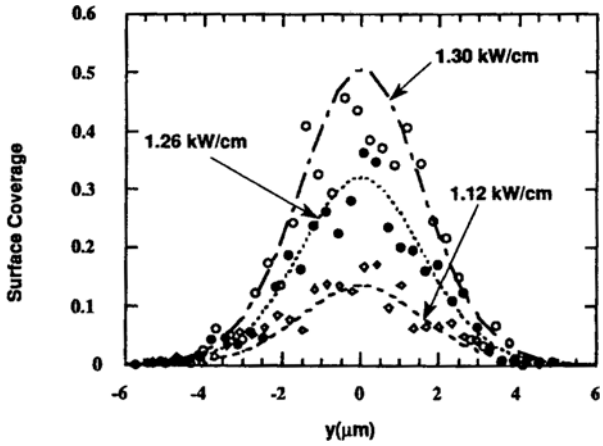

Fig. 6. Surface coverage distribution by particles across the lines shown in Fig. 3.

activation energy on aluminum surfaces obtained by thermal CVD (~17.8 kcal/mole) [Dubois et al., 1990]. This value is lower than those obtained on a silicon surfaces (25 kcal/mole), supporting the experimental observation [Han and Jensen, 1994] that overall growth rates on noble metal surfaces are higher than those on silicon surfaces.

The nucleation activation energy on oxide surfaces appeared to be so much higher than those on silicon or metal surfaces, that the use of high scan speeds or low laser powers did not produce any appreciable nucleation. Generally, the nucleated particles on SiO_2 surfaces are sparsely distributed and substantially bigger (few microns in diameter) than those observed on silicon surfaces. This behavior indicates that the increase in particle size is not by coalescence but by growth, and hence the relation for particle number distribution given by Eq. (10) or the relation for surface coverage distribution given by Eq. (17) may be used to obtain the nucleation kinetics on SiO_2 surfaces.

The nucleation study on SiO_2 was, however, not successful. The particles created on the SiO_2 surface were so randomly distributed along the laser scan directing that any statistical analysis of the particle distribution [such as, Eq. (10), (11), or (17)] would be meaningless. Also, because of the thermal insulation effect of the SiO_2 layer, once a stable nucleus was formed, its

Table 1. Nucleation kinetics for chemical vapor deposition of aluminum

Nucleation kinetics \ Al Precursors		TIBA[1]	TMAA[2,3]	DMEAA
Activation energy (kcal/mol)	on metal	27.7-32.6	17.8	17.8 or less
	on Si	73.5	--	**25.0**
	on SiO_2	91.9		
Induction time			10^{3} sec (on Si)	10^{-2} sec (on metals, Si, SiO_2)
Threshold temperature		-	103°C (on Si)	

References: (1) Lee et al., 1992; (2) Dubois et al., 1990; and (3) Foulon et al., 1993.

surface temperature increased sharply and accelerated the homogeneous growth on the nuclei. Consequently, before reaching a meaningful particle distribution, the big particles agglomerated with each other and formed a continuous line, which could not be used for the nucleation study.

Aluminum depositions by thermal CVD is in general sensitive to the type of the substrate surface, suggesting that the initial nucleation is a critical factor determining the properties of the resulted aluminum deposits. The kinetic information on the nucleation from DMEAA, obtained in this study, is compared with the published results from other aluminum precursors in Table 1. Nucleation activation energies (E_N) on metal surfaces were assumed to be the same as the growth activation energy on aluminum surface in all cases. For aluminum deposition from TIBA, many researchers [Tsao et al., 1984; Higashi, 1989; Lee et al., 1992] have found the selective deposition behavior toward metal surfaces in the presence of silicon or SiO_2. Also, in the case of silicon and SiO_2 surfaces, the deposition was found selective toward silicon. These observations follow exactly the trends in the E_N's on different surfaces listed in Table 1.

Little is known about aluminum nucleation from alane precursors, except for the E_N on metal surface [Dubois et al., 1990] and the induction time and threshold temperature for nucleation on silicon surfaces [Foulon and Stuke, 1993] for TMAA. The barriers for nucleation on a metal surface from the aluminum precursor used in this thesis, DMEAA, is presumably close to that from TMAA (17.8 kcal/mole), perhaps slightly lower because of the shift in the rate determining step [Han and Jensen, 1994]. By comparing the E_N on metal surface with the E_N on silicon surface (25.0 kcal/mole), one can expect the selective deposition toward metal surfaces in the presence of silicon, and indeed the selective behavior has been experimentally observed from the alane precursors [Simmonds et al., 1991; Han and Jensen, 1994]. However, the difference in E_N's on silicon and SiO_2 is not clear. Although, in this study using DMEAA, it appeared that E_N is lower on silicon than SiO_2, some have found the selectivity toward SiO_2 from TMAA[Baum et al., 1989; Gross et al., 1990]. A quantitative analysis is required to understand the selectivity between silicon and SiO_2 surfaces.

CONCLUSION

A new method of using LCVD to obtain nucleation kinetic information has been developed. It has been successfully applied to aluminum nucleation on (100)Si by LCVD from DMEAA. The nucleation induction time and nucleation activation energy on the silicon surface were estimated to 20 msec and 25 kcal/mole, respectively. By comparing the nucleation kinetics on silicon surfaces with those on metal surfaces, it was demonstrated that the selective behavior observed during experiments was caused by the differences in the nucleation activation energies on different types of substrate surfaces. The approach developed in this paper could however not be applied to SiO_2/Si substrates, because of the complexity involved with the insulating effect of the SiO_2 layer.

NOMENCLATURE

a_0 : jump distance of the absorbed monomer (approximately equal to the lattice parameter of the substrate)
E_a : activation energy for desorption
E_d : activation energy of surface diffusion
E_i : dissociation energy of a cluster containing i atoms into i adsorbed monomers
E_G : activation energy for growth
E_m : activation energy for monomer formation
E_N : activation energy for nucleation
F : fraction of the substrate surface covered by the particles ($0 \le F \le 1$)
i : number of monomers in a critically sized aggregate
k_m : pre-exponential factor for monomer formation
k_N : pre-exponential factor for nucleation
N_{obs} : actual number of particles after coalescence
N_0 : density of monomer adsorption site
N_P : number of stable particles with arbitrary sizes per unit area [#/cm^2]
N_∞ : number of critical nuclei created per laser scan [#/cm^2]
r_m : rate of formation of monomers on the substrate surface [#/cm^{2}s]
r_N : rate of formation of critical nuclei [#/cm^{2}s]
r_C : rate of decrease in total number of particles due to coalescence [#/cm^{2}s]
r_G : radial growth rate [cm/sec]
T_s : surface temperature
T_i : threshold temperature for nucleation
t_N : the time until each particle is born
v_x : laser scan speed
x : direction parallel to the laser scan
x_N : position along x-axis where each particle is born
y : direction perpendicular to the laser scan
$\overline{\phi^2}$: geometric average of ϕ_j^2
ϕ_j : radius of jth particle
ϕ_N : radius of the critical nucleus
φ : available cluster periphery for impingement
ν_1 : attempt frequency of the adsorbed monomer for desorption
ω : radius of incident laser spot

REFERENCES

Baum, T. H., Larson, C. E. and Jackson, R. L., "Laser-induced

Chemical Vapor Deposition of Aluminum", *Appl. Phys. Lett.*, **55**, 1264 (1989).

Dubois, L. H., Zegarski, B. R., Kao, C.-T. and Nuzzo, R. Z., "The Adsorption and Thermal Decomposition of Trimethylamine Alane on Aluminum and Silicon Single Crystal Surfaces: Kinetic and Mechanistic Studies", *Surf. Sci.*, **236**, 77 (1990).

Foulon, F. and Stuke, M., "Argon-ion laser direct-write Al Deposition from Trialkylamine Alane Precursors", *Appl. Phys. A*, **56**, 283 (1993).

Gross, M. E., Harriott, L. R. and Opila, R. L., Jr., "Focused Ion Beam Stimulated Deposition of Aluminum from Trialkylamine Alane", *J. Appl. Phys.*, **68**, 4820 (1990)

Han, J. and Jensen, K. F., "Pyrolytic Laser Assisted Chemical Vapor Deposition of Al from Dimethylethylamine-alane: Characterization and a New Two-step Writing Process", *Appl. Phys. Lett.*, **64**, 425 (1994).

Higashi, G. S., "The Chemistry of Alkyl-aluminum Compounds During Laser-assisted Chemical Vapor Deposition", *Appl. Surf. Sci.*, **43**, 6 (1989).

Kim, D.-H, Lee, I.-J., Rhee, S.-W. and Moon S. H., "Effect of Fluorine Chemistry in the Remote Plasma Enhanced Chemical Vapor Deposition of Silicon Films from Si_2H_6-SiF_4-H_2", *Korean J. of Chem. Eng.*, **12**, 572 (1995).

Lax, M., "Temperature Rise Induced by a Laser Beam II. The Nonlinear Case", *Appl. Phys. Lett.*, **33**, 786 (1978).

Lee, J. H., Moon, S. H. and Rhee, S.-W., "Simulation of Silicon Film Growth by Silane Decomposition at Low Pressures and Temperatures", *Korean J. of Chem. Eng.*, **9**, 29 (1992).

Lee, K. I., Kim, Y. S. and Joo, S. K., "Effect of Substrate Temperature on the Selectivity in Low Pressure Chemical Vapor Deposition of Aluminum", *J. Electrochem. Soc.*, **139**, 3578 (1992).

Rantala, T. T. and Levoska, J., "A Numerical Solution Method for the Laser-induced Temperature Distribution", *J. Appl. Phys.*, **65**, 4475 (1989).

Simmonds, M. G., Phillips, E. C., Hwang, J. and Gladfelter, W. L., "A Stable, Liquid Precursor for Aluminum", *Chemtronics*, **5**, 155 (1991).

Tsao, J. Y. and Ehrlich, D. J., "Patterned Photonucleation of Chemical Vapor Deposition of Al by UV-laser Photodeposition", *Appl. Phys. Lett.*, **45**, 617 (1984).

Venables, J. A., Spiller, G. D. T. and Hanbucken, M., "Nucleation and Growth of Thin Films", *Rep. Prog. Phys.*, **47**, 399 (1984).